Springer

Journal of Mechanical Science and Technology 23 (2009) 3005~3012

Journal of
Mechanical
Science and
Technology

www.springerlink.com/content/1738-494x
DOI 10.1007/s12206-009-0904-4

A robust sliding mode controller design for a ball screw table driven by an air motor †

Yu-Ta Shen[1,*], Yean-Ren Hwang[2] and Chia-Sheng Cheng[3]

[1]*Department of Mechanical Engineering, National Central University, Chung-Li, Taiwan 320*
[2]*Department of Mechanical Engineering and the Institute of Opto-Mechatronics Engineering, National Central University, Chung-Li, Taiwan 320*
[3]*Department of Mechanical Engineering, National Central University, Chung-Li, Taiwan 320*

(Manuscript Received October 16, 2008; Revised June 17, 2009; Accepted July 13, 2009)

Abstract

Air motors are often applied in the automation industry in areas with special requirements, such as in spark-prohibited environments, the mining industry, chemical manufacturing plants, and similar locations. The purpose of this study is to analyze the behaviors of a ball screw table powered by a vane-type air motor and to design a robust sliding mode controller for the inlet pressure. The rotational speed of the air motor is closely related to the pressure and flow rate of the compressed air. Furthermore, the compressibility of the air and the friction in the mechanism mean that the overall system is nonlinear, with fluctuating input. A robust sliding mode control is developed to overcome the effects of variations in the inlet pressure and air leakage problems. The experimental results validate the robustness of the proposed position control strategy.

Keywords**:** Air motor; Robust; Sliding mode controller

1. Introduction

Although electrical motors are still the main devices used in most manufacturing plants, air motors have attracted more and more attention over the past few decades because they are cheaper, safer, cleaner, smoother and more efficient (i.e., able to maintain a higher power to weight ratio) [1-4]. Moreover, the air motor is the only device that can be used in certain special locations, such as in spark-prohibited environments, in the mining industry, in chemical manufacturing plants, in vehicles, and storage facilities used for explosive materials.

In the air motor, the energy of compressed air is converted into mechanical energy. In general, the compressibility of air and the friction created by its mechanisms make air motors demonstrate highly nonlinear behaviors. However, the position control system of the air motor may show variable uncertainty from the control input of different pressures due to the applied input signal. Hence, it is difficult to design a position controller capable of realizing accurate position control at all times. To date, there has been a number of investigations and analyses of the dynamics of air motors carried out. For example, in the proportional integral (PI) controller, proposed by Zhang and Nishi [2], the all air motor system is considered as a first order linear system. Although the PI control algorithm is simple and highly-reliable when the PI values are adjusted very well, the performance of the PI controller is far from consistent because of the nonlinear speed characteristics of the air motor under different operating conditions. In a paper by Hwang, et al. [5], the mode reference adaptive control

† This paper was recommended for publication in revised form by Associate Editor Kyongsu Yi
*Corresponding author. Tel.: +886 3 4267342, Fax.: +886 3 4254501
E-mail address: klneclipse@yahoo.com.tw

(MRAC) was adopted for fuzzy control to eliminate the dead-zone caused by friction. The results of this study showed that the mode reference output could be tracked and that an accurate speed control performance was attainable. A fourth-order nonlinear mode was developed by Puan and Moore [6] utilizing parameters identified through experimental data. However, due to the complexity of this mode, the number of parameters was large, making the process of deriving parameters complicated and time consuming. Others have applied control schemes for guaranteeing accurate position control of pneumatic cylinders [7-9] which are subject to the uncertain dynamics of pneumatics. A method of fuzzy sliding mode position control incorporating a ball screw driven by an air motor has been proposed by Shin and Lu [10] in which fuzzy logic control was applied to avoid the disadvantages of disturbances and chattering.

Air motors have -unpredictable characteristics. In most practical motion systems, the inlet pressure to the air motor will decrease with each experimental run. The leakage of pressure is a problem for accurate position actuators as well as for industrial applications. Eliminating this problem in order to improve control performance is very important. Air motors suffer from a variable dead-zone when the input control pressure is variable. This makes it difficult to design a position controller which can achieve accurate position control at all times, and which takes into account the deterioration of the dynamic response of the system caused by the leaking pressure. We sought to overcome this problem by designing a position control scheme for an air motor which compensated for the pressure leakage. The proposed control scheme utilized a sliding mode control for a second-order uncertain system. This could decrease the chattering while preserving the robustness of the different inlet pressures and leaking pressure problems for a ball screw table. The experimental results confirmed the good performance of the control system in relation to different inlet operation pressures and the perfect steady state position error.

The remainder of the paper is organized as follows: the introduction to the air motor ball screw table system is described in Section 2; the nonlinear behaviors of the air motor system are analyzed in Section 3; the algorithm for the robust sliding mode control design is discussed in Section 4; the experimental results are shown in Section 5; and some conclusions are offered in Section 6.

2. Air motor ball screw table system

Fig. 1 shows a rough map of a vane-type air motor. The motor has a rotational drive shaft with four slots, each of which is fitted with a freely sliding rectangular vane. When the drive shaft starts to rotate, the vanes tend to slide outward due to the centrifugal force and are limited by the shape of the rotor housing. Depending on the flow direction, the motor will rotate in either a clockwise or counterclockwise direction. The difference in air pressure between the inlet and outlet provides the torque required to move the shaft. Hence, the higher the flow rate and the larger the pressure difference, the larger the torque on the shaft and the higher the rotational speed provided.

A schematic diagram of the air motor system is shown in Fig. 2. The system consists of an air motor

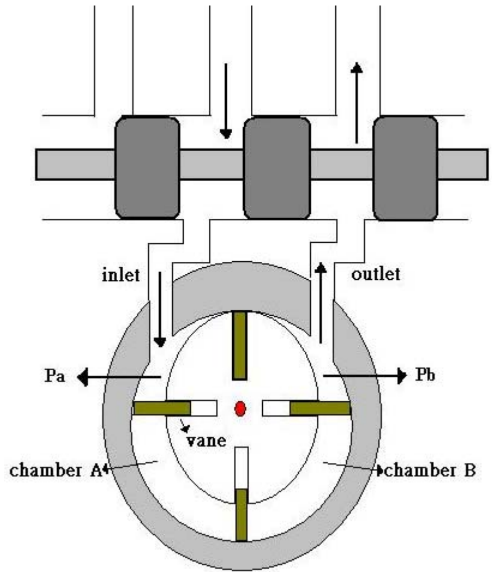

Fig. 1. Vane-type air motor.

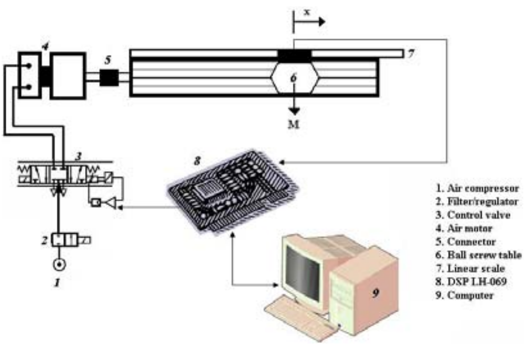

Fig. 2. Schematic diagram of the air motor system.

(GAST 1AM), an air tank, an electronic proportional directional control valve (FESTO MPVE), a filter/regulator with lubricant (SHAKO FRL-600), an optical linear scale (FUTABA FJH5515IDR) with an accuracy of 5 um, and a digital signal processor (DSP, TI C240). The airflow path starts from the air tank moving through the filter, then through the control valve, finally entering the air motor. The airflow entering the motor is determined by the valve position, which is controlled by an externally applied voltage, denoted by v. When v equals 5 V, the valve will stay in the middle and both left and right entries will be closed. The valve will move to the right when v is above 5 V, and becomes fully opened when v is equal to 10 V. Similarly, the valve will move to the left if v is less than 5 V, and will be fully opened at 0 V. The direction of the air motor depends on whether the voltage v is above or below 5 V. The control input from DSP denoted by u, will be converted into v as $v=u+5$. The experimental air motor ball screw table system is shown in the Fig. 3.

Fig. 3. Photograph of the experimental air motor system.

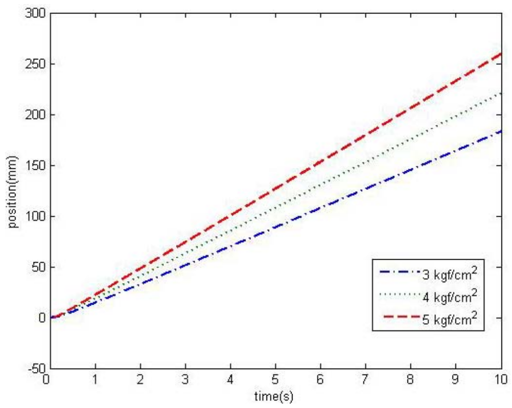

Fig. 4. The position responses with different inlet pressure.

3. Nonlinear behaviors of the air motor system

The rising time of the system is limited by the inlet pressure. A large inlet pressure brings about a fast system transition response. The rising times for different inlet pressures are shown in Fig. 4. There are various system parameters that affect the nonlinear characters, such as friction, air compressibility, and pressure leakage. We propose using a PID (proportional–integral–derivative) controller to control the position of the ball screw table in order to describe these behaviors. Fig. 5 shows the results in relation to the parameters of the PID controller. E_{ss} is in the steady state error. The results are: Kp=16.2, KI=0.01, KD=0.34; and the inlet pressure is constant. The three different position curves represent the results of three experimental runs with the same inlet pressure. It is obvious that these three position curves have different rise times and steady state errors. These results suggest that the robustness of the PID control is not sufficient for this nonlinear system. Even when the parameters of the PID control were modulated to maintain a constant inlet pressure, the system did not show evidence of precise steady state error. If the operating point (inlet pressure) of the system changes, it is hard to maintain accurate performance simply with PID control. Since the purpose of this study is to control the position of the system given different inlet pressures, we cannot overemphasize the importance of the robustness. Thus, we adopt the sliding mode control for second-order uncertain systems to overcome system nonlinearity and to guarantee robustness for various inlet pressures (the inlet pressure is restricted to 3 - 5 kgf/cm^2).

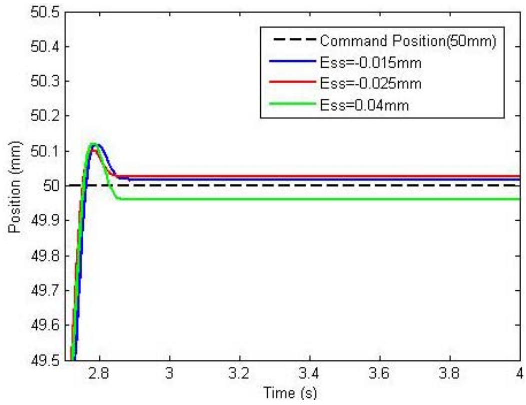

Fig. 5. Experimental results attained by the PID controller with the same inlet pressure.

4. A robust sliding mode control for second-order uncertain systems: controller design

A sliding mode controller is designed to maintain the robust performance of the air motor by overcoming variations in the inlet pressure and nonlinear disturbances of the air. The air motor is connected to a ball screw table to form a second-order system, as shown in Figs. 1 and 2. The dynamics of the system can be described by the following equation which considered friction:

$$\mathrm{A}\left(P_a - P_b\right) + D_{ex} = \mathrm{M}\ddot{\mathrm{x}} + \mathrm{C}_{\mathrm{vis}}\dot{\mathrm{x}} + \mathrm{C}_{\mathrm{cou}}\mathrm{sign}(\dot{\mathrm{x}}) \,, \quad (1)$$

where $\mathrm{A}\left(P_a - P_b\right)$ is the input force (A is the area of the sliding rectangular vane in the air motor); D_{ex} is the external disturbance; M is the total mass of the air motor and the table; C_{vis} is the viscous friction coefficient; and C_{cou} is coulomb friction.

Eq. 1 can be derived as:

$$\ddot{\mathrm{x}} + \frac{\mathrm{C}_{\mathrm{vis}}}{\mathrm{M}}\dot{\mathrm{x}} = \frac{1}{\mathrm{M}}\left[\mathrm{A}\left(P_a - P_b\right) + D_{ex}\text{-}\mathrm{C}_{\mathrm{cou}}\mathrm{sign}(\dot{\mathrm{x}})\right]. \quad (2)$$

In order to facilitate the controller design, the overall system can be described by:

$$\begin{aligned} &\ddot{x} + a(t)\dot{x} = b(t)\left[u + d(t)\right] \\ &\ddot{x} = -a(t) + b(t)u + b(t)d(t) \end{aligned} \,, \quad (3)$$

where $a(t) > 0,\ b(t) > 0$ are system variables; and $d(t)$ represents the summation of the disturbance and nonlinear friction. It is assumed that:

$$\begin{aligned} &\beta_{\min} \le b^{-1}(t) \le \beta_{\max} \\ &\alpha_{\min} \le b^{-1}(t)a(t) \le \alpha_{\max} \,. \\ &d(t) < D \end{aligned} \quad (4)$$

The inlet pressure is restricted to within 3 to 5 kgf/cm^2 so that the beta_min, beta_max, alpha_min, and alpha_max are positive numbers and determined by the inlet pressure segment D>0.

The reference input is r and the tracking error can be defined as

$$e = x - r \,. \quad (5)$$

The sliding mode surface is chosen as follows:

$$s = \dot{e} + ce \,, \quad (6)$$

where c is the slope of the surface. We now define a Lyapunov function $V = \frac{1}{2}s^2$. Eq. (7) can now be derived from Eq. (6) by

$$\begin{aligned} \dot{s} &= \ddot{e} + c\dot{e} = \ddot{x} + c\dot{x} - (\ddot{r} + c\dot{r}) \\ &= \ddot{x} + c\dot{x} + R \end{aligned} \,, \quad (7)$$

where $R = -(\ddot{r} - c\dot{r})$. By substituting Eq. (3) into Eq. (7) we get

$$\begin{aligned} \dot{s} &= -a\dot{x} + c\dot{x} + bu + bd + R \\ &= b\left[-b^{-1}a\dot{x} + b^{-1}c\dot{x} + b^{-1}R + u + d\right] \end{aligned}. \quad (8)$$

$$b^{-1}\dot{s} = -b^{-1}a\dot{x} + b^{-1}c\dot{x} + b^{-1}R + u + d \,. \quad (9)$$

The designed control input is

$$u = u_{eq} + u_{vss} \,, \quad (10)$$

where u_{eq} is the equivalent control input for no disturbance and u_{vss} is the robust control input for a disturbance. These two control inputs are designed to let the system converge to the original point. The u_{eq} and u_{vss} are designed as follows:

$$\begin{aligned} &u_{eq} = \hat{\alpha}\dot{x} - \hat{\beta}c\dot{x} - \hat{\beta}R \\ &u_{vss} = -\Sigma \cdot sign(s) \end{aligned} \,, \quad (11)$$

where:

$$\begin{aligned} &\hat{\alpha} = \frac{\alpha_{\max} + \alpha_{\min}}{2} \\ &\hat{\beta} = \frac{\beta_{\max} + \beta_{\min}}{2} \end{aligned} \,, \quad (12)$$

Eq. (10) can now be written as:

$$u = \hat{\alpha}\dot{x} - \hat{\beta}c\dot{x} - \hat{\beta}R - \Sigma \cdot sign(s) \,.$$

Substituting Eq. (10) into Eq. (9) we get:

$$\begin{aligned} b^{-1}\dot{s}s &= -b^{-1}a\dot{x}s + b^{-1}c\dot{x}s + b^{-1}Rs + \hat{\alpha}\dot{x}s \\ &\quad - \hat{\beta}c\dot{x}s - \hat{\beta}Rs - \Sigma \cdot |s| \\ &= (\hat{\alpha} - b^{-1}a)\dot{x}s + (b^{-1} - \hat{\beta})c\dot{x}s \\ &\quad + (b^{-1} - \hat{\beta})Rs - \Sigma \cdot |s| \end{aligned} \,. \quad (13)$$

From Eq. (2), the following equation can be obtained:

$$\begin{aligned} b^{-1}\dot{s}s &= (\hat{\alpha} - b^{-1}a)\dot{x}s + (b^{-1} - \hat{\beta})c\dot{x}s \\ &\quad + (b^{-1} - \hat{\beta})Rs - \Sigma \cdot |s| \\ &\le \Delta\alpha|\dot{x}||s| + \Delta\beta|c\dot{x}||s| \\ &\quad + \Delta\beta|R||s| + D - \Sigma \cdot |s| \end{aligned}, \tag{14}$$

where

$$\Delta\alpha = \frac{\alpha_{\max} - \alpha_{\min}}{2}, \quad \Delta\beta = \frac{\beta_{\max} - \beta_{\min}}{2}. \tag{15}$$

If Σ is chosen to satisfy the following conditions:

$$\Sigma = \Delta\alpha|\dot{x}||s| + \Delta\beta|c\dot{x}||s| + \Delta\beta|R||s| + D + \sigma, \quad \sigma > 0 \tag{16}$$

and

$$b^{-1}\dot{s}s \le -\sigma|s|, \tag{17}$$

then it can be proven that $\dot{V} \le 0$. Eq. (17) shows that the design of the control input satisfies the approaching sliding condition, and thus ensures that the system will converge to the point of origin.

In order to improve the chattering, the $sign(s)$ function can be changed to an $sat(s)$ function (saturation function) as in Eq. (11).

$$u = \hat{\alpha}\dot{x} - \hat{\beta}c\dot{x} - \hat{\beta}R - \Sigma \cdot sat(s), \tag{18}$$

where

$$\Sigma = \Delta\alpha|\dot{x}||s| + \Delta\beta|c\dot{x}||s| + \Delta\beta|R||s| + D + \sigma, \quad \sigma > 0.$$

Generally speaking, to eliminate the chattering phenomenon in the boundary layer, the design of the $sat(s)$ function is usually a linear function. However, it was found that the system had slight chattering when a linear function was used. Hence a cubic function was adopted to replace the linear function, as shown in Fig. 6. The sliding surface can approach swiftly and the movement on the sliding surface is smooth. The simulated and experimental position control results are shown in Figs. 7 and 8, respectively, where P_{ss} is the steady state position. The blue line indicates the $sat(s)$ function (linear function). It has a 0.05% chattering phenomenon. The red line indicates the adoption of a cubic function. It has a smooth performance with a steady state error of under 0.01%. It can be seen that the cubic function can more effectively reduce the chattering phenomenon.

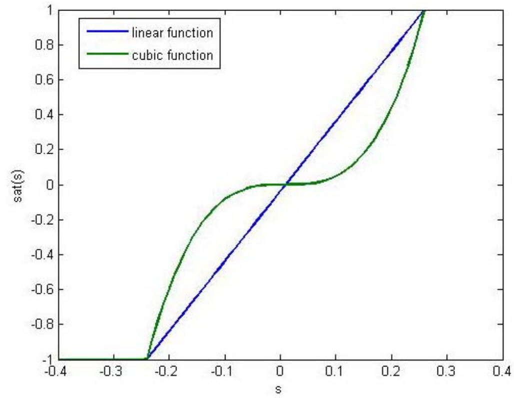

Fig. 6. Saturation function.

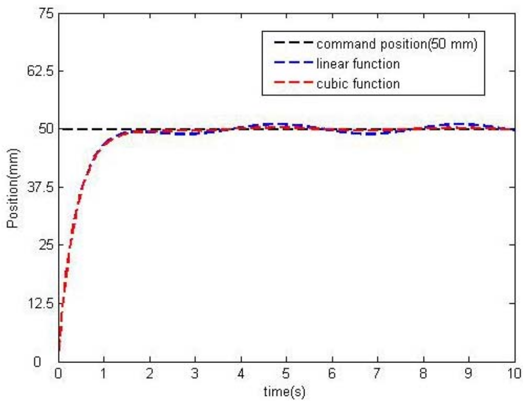

Fig. 7. Simulated results for the linear and cubic saturation functions.

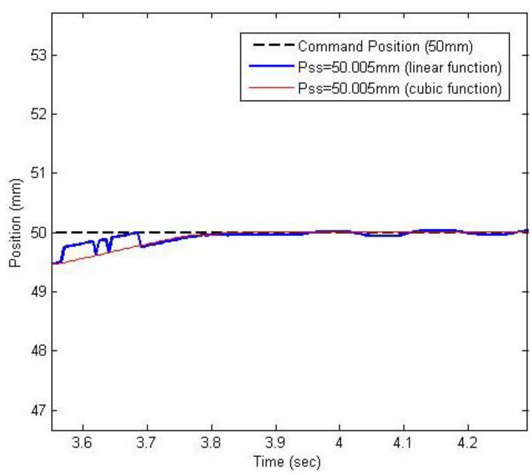

Fig. 8. Experimental position results of the sliding mode control for the linear and cubic saturation functions.

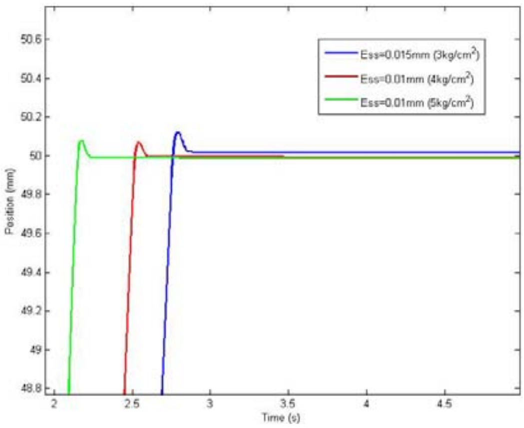

Fig. 9. Experimental results of the PID position control.

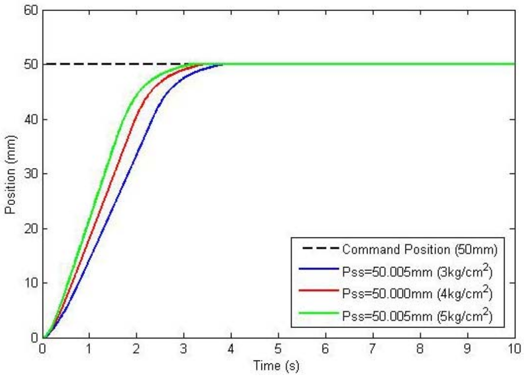

Fig. 10. Experimental results of the sliding mode position control under the no-loading condition.

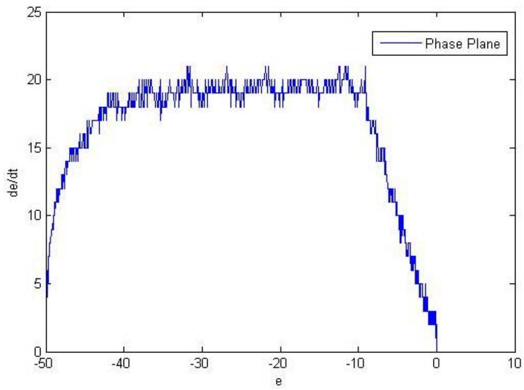

Fig. 11. Experimental results of the sliding mode phase plane.

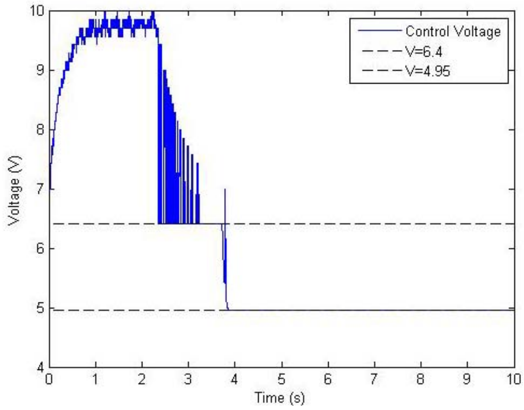

Fig. 12. Experimental results of the sliding mode control input with inlet pressure of $3kg/cm^2$.

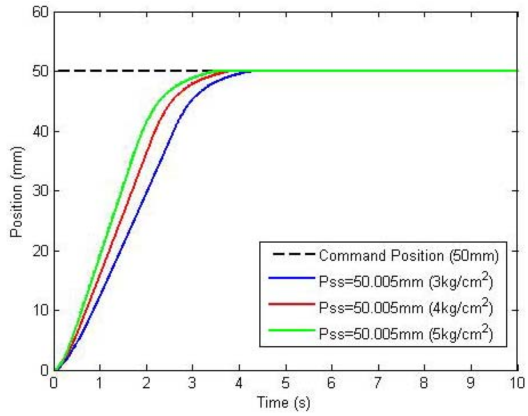

Fig. 13. Experimental results of the sliding mode position control under the loading mass of 10 kg.

5. Experimental results

The controller design described above was applied to an air motor ball screw table system. The PID controller was found to be not robust enough for various inlet pressures. The inlet pressures used in the experiments were $3kg/cm^2$, $4kg/cm^2$ and $5kg/cm^2$. The experimental results for the PID controller show that the steady state errors were about 0.01- 0.015mm (see Fig. 9). The low inlet pressure had a large error and the overshoot associated with each inlet pressure could not be eliminated by the large gains of the PID controller necessary to maintain the rise time of the system. In this study, a sliding mode controller to achieve robust control of an air motor ball screw table system was implemented. The experimental results (under the no-loading conditions) are shown in Fig. 10. There was no serious overshoot with our system and the steady state errors were 0.005mm, 0mm, and 0.005mm, respectively. The e (error) and $\dot{e}$ converged to the point of origin, as can be seen in Fig. 11. The control input (inlet pressure $3kg/cm^2$) is shown in Fig. 12. The experimental results illustrate the excellent performance of the robust sliding mode controller (with the cubic saturation function) for different inlet pressures which reduced the chattering phenomenon. Fig. 13 shows the results for a position control with a loading mass of 10 kg. It is obvious that the steady state error can be restrained to 5 um or less. The setting time is about 4.2 s with an inlet pressure of $3kg/cm^2$, as compared to 4 s under the no-loading conditions as shown in Fig. 10. Clearly, even under the loading conditions, the system produces accurate results.

6. Conclusions

In this study, we developed a robust sliding mode controller for an air motor ball screw table. These systems usually suffer from problems of nonlinearity due to variations in the compressibility of air. When inlet pressures vary, the variables of the system will change, making the traditional PID controller unsuitable. The more robust sliding controller design of this study, however, provides very good traction performance for different inlet pressures. Even in systems with air leakage problems, the adopted controller shows improved performance (the cubic saturation function) as well as effective reduction in the chattering phenomenon. The experiment results clearly show that our system has very strong robustness under the loading conditions. The steady state error decreased and system chattering was eliminated.

References

[1] R. Richardson, M. Brown, B. Bhakta and M. Levesley, Impedance control for a pneumatic robotbasedaround pole-placement, joint space controllers, Control. Eng. Pract. 13 (3) (2005) 291-303.

[2] Y. Zhang and A. Nishi, Low-pressure air motor for wall-climbing robot actuation, Mechatronics 13 (4) (2003) 377-392.

[3] S. R. Pandian, F. Takemura,, Y. Hayakawaand and S. Kawamura, Control performance of an air motorcanair motors replace electric motors?, IEEE Int.Conf. on.1 (1999) 518–524.

[4] M. O. Tokhi, M. Al-Miskiryand and M. Brisland, Realtime control of air motors using a pneumatic Hbridge,Control. Eng. Pract. 9 (4) (2001) 449-457.

[5] Y. R. Hwang, Y. D. Shen and K. K. Jen, Fuzzy MRAC controller design for vane-type air motor systems, J. of Mech. Sci. and Tech.22, (3) (2008) 497- 505.

[6] J. Wang, J. Puand P. and R. Moore, Modelling study and servo-control of air motor systems, Int. J. Control.71 (3) (1998) 459- 476.

[7] J. Song and Y. Ishida, A robust sliding mode control for pneumatic servo systems, Int. J. Eng. Sci. 35 (8) (1997) 711-723.

[8] Ž. Šitum, T. Žilić and M. Essert, High speed solenoid valves in pneumatic servo applications, 2007 Mediterranean Conf on Control and Automation. (2007) 1-6.

[9] T. Nguyen, J. Leavitt, F. Jabbari and J. E. Bobrow, Accurate sliding-mode control of pneumatic systems using low-cost solenoid valves, IEEE/ASME Trans on Mechatronics, 12 (2) (2007).

[10] M. C. Shin and C. S. Lu, Fuzzy sliding mode position control of a ball screw driven by pneumatic servomotor, Mechatronics. 5 (4) (1995) 421-431.

Shen, Yu-Ta received his BS degree in Mechanical Engineering from Yuan Ze University in 2004 and studies P.H.D degree in National Central University from 2004 to now. His current research topics include sliding model control on the pneumatic device and fuel cell controller development.

Hwang, Yean-Ren received his BS degree in Mechanical Engineering from National Taiwan University in 1983, master degree from Georgia Institute of Technology in 1986 and Ph.D. degree from University of California at Berkeley in 1993. His current research topics include nonlinear dynamics and control, machine vision and development of fuel cell and air power motorcycles.

Cheng, Chia-Sheng received his BS degree in Mechanical Engineering from Chung Yuan Christian University in 2006 and M.S degree from National Central University in 2008. His research topics is sliding model control on the pneumatic device.